Inorganic Chemistry

ARTICLE

pubs.acs.org/IC

Two Stage Magnetic Ordering and Spin Idle Behavior of the Coordination Polymer $Co_3(OH)_2(C_4O_4)_2 \cdot 3H_2O$ Determined Using Neutron Diffraction

Richard A. Mole,[†] John A. Stride,[‡] Paul F. Henry,[§,◆] Markus Hoelzel,[∥] Anatoliy Senyshyn,[∥] Antonio Alberola,[⊥] Carlos J. Gómez Garcia,[#] Paul R. Raithby,[▽] and Paul T. Wood*[,○]

[†]Forschungsneutronenquelle Heinz Maier Leibnitz (FRM II), Technische Universität München, Lichetenbergstrasse 1, 85747 Garching, Germany

[‡]School of Chemistry, University of New South Wales, Sydney 2052, Australia

[§]Institut Laue-Langevan, BP 156, 6 Rue Jules Horowitz, 38042 Grenoble Cedex 9, France

[∥]FB Material- und Geowissenschaften, Fachgebiet Strukturforschung, Technische Universität, Darmstadt, Petersenstrasse 23, D-64287 Darmstadt, Germany

[⊥]Dpto. de Quimica Fisica y Analitica, Universitat Jaume I, Avda. Sos Baynat s/n, 12071 Castellón, Spain

[#]Instituto de Ciencia Molecular, Universidad de Valencia, Pol. La Coma s/n, 46980 Paterna, Valencia, Spain

[▽]Department of Chemistry, University of Bath, Bath, BA2 7AY, U.K.

[○]University Chemical Laboratory, University of Cambridge, Lensfield Road, Cambridge, CB2 1EW, U.K.

Supporting Information

ABSTRACT: We report the magnetic structure of two of the magnetically ordered phases of $Co_3(OH)_2(C_4O_4)_2 \cdot 3H_2O$, a coordination polymer that consists of a triangular framework decorated with anisotropic Co(II) ions. The combination of neutron diffraction experiments and magnetic susceptibility data allows us to identify one phase as displaying spin idle behavior, where only a fraction of the moments order at intermediate temperatures, while at the lowest temperatures the system orders fully. This novel magnetic behavior is discussed within the framework of a simple Hamiltonian and representational analysis and rationalizes this multiphase behavior by considering the combination of frustration and anisotropy.

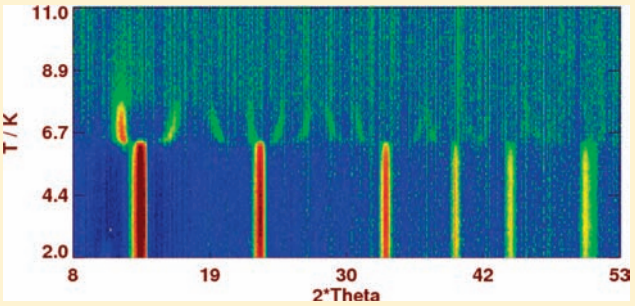

INTRODUCTION

Coordination polymers, also known as metal organic frameworks (MOFs), have become one of the most active areas of inorganic materials chemistry.[1−3] This is largely because of their proposed use as solid supports in the fuel tanks of hydrogen powered vehicles.[4] The need to characterize the binding sites of H_2 molecules to the walls of the host has led to the use of neutron diffraction[5−7] and scattering[8,9] techniques on a range of porous MOFs. There has also been considerable interest in the magnetism of coordination polymers because the anisotropy of their lattices can lead to exotic magnetic behavior,[10] while structures have also been shown to be dependent on the level of hydration, indicating that this parameter could possibly be used to manipulate the magnetic behavior. However, a complete understanding of their magnetism has been hampered because of the difficulty of in-depth studies. In contrast, exotic states in metal oxides have been very well characterized by a combination of techniques such as diffraction[11] and inelastic scattering[12] of neutrons, and muon spectroscopy.[13] Neutron techniques have been assumed to be unsuitable for magnetic MOFs because of the incoherent scattering from ^1H and the difficulty of deuterating these compounds. In this respect, coordination networks incorporating the squarate dianion are promising candidates for study as the ligand contains no "organic" hydrogen. We have already reported on the neutron diffraction[14] and inelastic neutron scattering[15] of $Mn_2(OH)_2(C_4O_4)$,[16] where the magnetization behavior is relatively simple. The material $Co_3(OH)_2(C_4O_4)_2 \cdot 3H_2O$ (**1**), previously reported by us,[17] and further studied by Kepert, Kurmoo and coworkers,[18] is a perfect candidate for further study as it shows complex magnetic behavior and is susceptible to deuteration by exchange with D_2O. Here we report the magnetic susceptibility and neutron diffraction data of a polycrystalline sample of **1**, prepared using a modification of the original synthesis.

EXPERIMENTAL SECTION

Synthesis. In the Teflon insert of a 23 mL Parr reactor, $Co(OAc)_2 \cdot 4H_2O$ (250 mg, 1 mmol) was dissolved in water (5 mL). Aqueous KOH (2 mL of a 2 M solution, 4 mmol) was added followed by solid squaric acid

Received: September 16, 2010
Published: February 04, 2011

Table 1. Crystal Data and Structure Refinement for 1 at 30 K

empirical formula	$C_8H_8Co_3O_{13}$
crystal system	monoclinic
space group	*C2/m*
formula weight (g/mol)	488.93
a (Å)	9.2711(4)
b (Å)	12.8719(6)
c (Å)	5.4940(2)
β (deg)	90.685(2)
volume (Å^3)	655.59(5)
Z	2
$R_1 I > 2\sigma(I)$	0.0338
wR_2 indices (all data)	0.0857

(329 mg, 2.88 mmol) followed by further water (2.5 mL). The autoclave was sealed and heated to 200 °C for 15 h followed by cooling to about 50 °C over 4 h before opening. The product was then isolated by filtration to yield 100 mg 60%. Deuteration was performed by cycles of dehydration by heating to 150 °C under vacuum, followed by exposure to D_2O vapor under a flow of nitrogen. This was repeated for five cycles.

Diffraction. Single crystal X-ray diffraction was performed using a Bruker Kappa CCD diffractometer equipped with an Oxford Cryosystems Helix crystal cooling device operating at 30 K. CCDC-735274 contain supplementary crystallographic data for this paper. These data can be obtained free of charge from The Cambridge Crystallographic Data Centre via www.ccdc.cam.ac.uk/data_request/cif.

All neutron diffraction experiments were performed using a 2.5 g sample in a standard vanadium sample can. A standard orange cryostat was used with the D20 and D2B diffractometers at the Institut Laue Langevin (ILL), Grenoble, France, while those on the SPODI diffractometer at the Forschungsnutronenquelle Heinz Maier-Liebnitz (FRM II), Munich, Germany, used a CCR system. Wavelengths used were 2.5 Å (D20), 1.594 Å (D2B), and 2.537 Å (SPODI). Standard corrections for detector efficiency were performed in all cases. For SPODI and D2B data the Debye−Scherrer rings were straightened to allow the use of a large area of the detector. Rietveld refinements[19] were performed using the GSAS suite of programs while the magnetic structures were calculated using the SARAh representational analysis software.[20]

Magnetic susceptibility measurements were performed using a Quantum Design MPMS-XL-5 magnetometer with the samples isolated in gelatin capsules. Direct current (DC) magnetization measurements were performed in the range 2−300 K with a 100 Oe measuring field, while alternating current (AC) measurements were performed with an alternating field of 3.95 Oe in the temperature range 1.8−10 K at 110 Hz with a range of different DC magnetic fields applied (7−700 Oe).

RESULTS

Crystal Structure. The crystal structure of compound **1** is already known over a wide temperature range >100 K;[18] however, for this study we needed to be assured that there were no significant structural changes at temperatures close to the magnetic ordering. Additional data was collected at 30 K, and the structure determination repeated (Table 1); this revealed no significant change from the room temperature study both in the framework and, more importantly, to the disorder of the guest water molecules. To understand the magnetic behavior of **1** we first need to consider the possible pathways for magnetic superexchange. The important structural features are as follows: μ_3-OH bridged isosceles triangles of cobalt atoms share alternating edges and vertices to form $Co_3(OH)$ strips parallel to the *c* axis forming the backbone of the lattice (Figure 1). Both cobalt ions

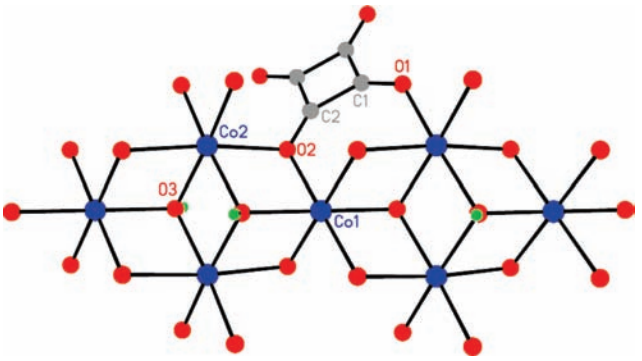

Figure 1. Section of the alternating edge and vertex sharing chain in **1**, from X-ray data, showing the possible bridging interactions.

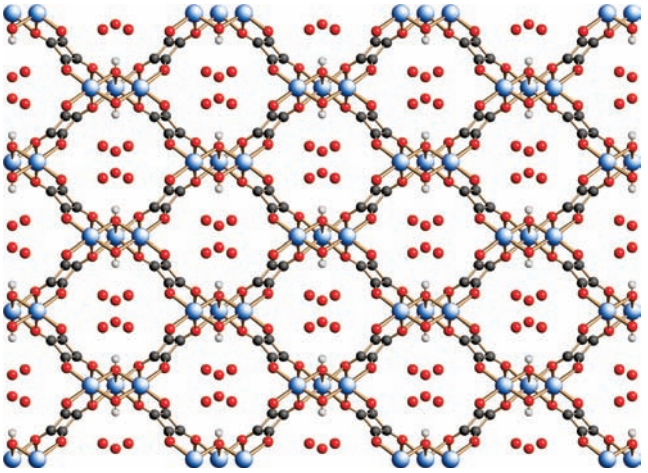

Figure 2. Packing diagram of **1** along the crystallographic *c* axis, showing the large water filled channels.

have a distorted octahedral coordination environment and are further bridged by squarate dianions via both a one atom (M−O−M) and a four-atom (M−O−C−C−O−M) bridge. The squarate dianion also facilitates four and five atom bridges to neighboring strips resulting in the formation of large water-filled channels (Figure 2). As shorter superexchange pathways mediate the strongest spin−spin interactions, it is anticipated that these long bridging pathways between strips will be relatively weak.

Magnetometry. We were initially suspicious of the unusual nature of the susceptibility, with three Néel point-like discontinuities in a small temperature range (Figure 3). This result was subsequently confirmed from three independent samples on two different magnetometers and by checking sample purity by X-ray powder diffraction (Figure S1, Supporting Information). At 8 K there is a discontinuity, followed by two maxima at 5.7 and 3.2 K. Fitting the data between 20 and 300 K to the Curie−Weiss law yields $C = 10.58(1)$ cm^3 mol^{-1} K and $\Theta = -5.6(2)$ K. The room temperature value of χT is 10.3 cm^3 mol^{-1} K consistent with the observed Curie constant and within the range expected for three Co^{2+} ions. Using a spin only approach, one can extract an effective *g* value of 2.7, this is similar to other values reported in the literature using this oversimplified approach.[21]

The application of Mean Field Theory to the Weiss constant is not a good measure of coupling strength here as it is unsuitable for anisotropic systems, and in this case it will also include a component due to zero field splitting[22] as a result of the spin-orbit coupling

dx.doi.org/10.1021/ic101897a |*Inorg. Chem.* 2011, 50, 2246–2251

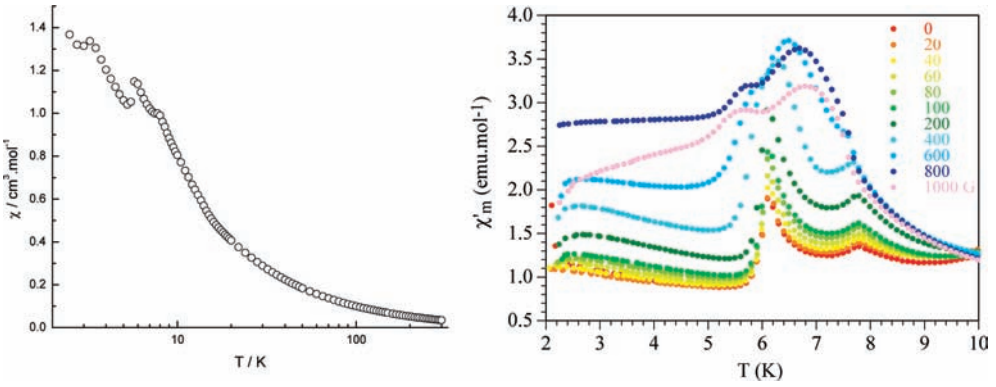

Figure 3. Left, DC susceptibility of **1** in a measuring field of 100 Oe; right, AC susceptibility in a range of DC fields (inset-size of DC field in Oe).

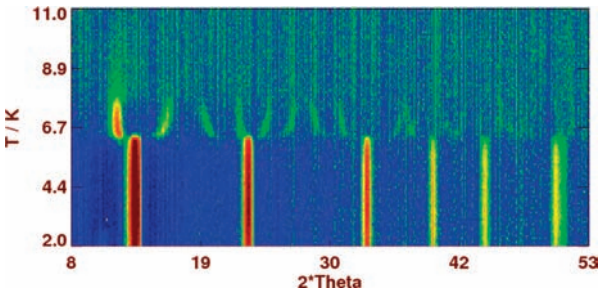

Figure 4. Temperature dependence of the magnetic diffraction in **1** obtained by subtracting the 12 K diffraction pattern from the raw data.

inherent with the unquenched orbital angular momentum associated with the electronic configuration of octahedral Co(II). We have also recorded AC susceptibility data in varying static applied fields; the temperature dependence of χ' confirms the presence of three different ordered phases and shows that with an applied field of over 7000 Oe all three phase transitions are suppressed.

Neutron Diffraction. Neutron diffraction data were collected using the high flux diffractometer D20 at the ILL.[23] At approximately 8 K, extra Bragg reflections are observed, characteristic of a magnetic phase transition (Figure 4). The positions of several of these new peaks show a strong temperature dependence; this behavior is indicative of an incommensurate magnetic structure, that is, the magnetic unit cell is not an integer multiple of nuclear cells. Below 5.75 K a second set of magnetic Bragg peaks is observed with positions that do not vary as a function of T as the sample is cooled down to 2 K. Integration over the 2θ range of individual magnetic Bragg peaks and plotting as a function of temperature shows that there are three changes in intensity, consistent with three magnetic phase transitions, with the final one occurring at 3.25 K; these intensity changes correspond to the three different discontinuities in the susceptibility (Figure 5) giving rise to four different magnetic regimes labeled **A**, **B**, and **C** for the regions below 3.25 K, between 3.25 and 5.75 K, between 5.75 and 8 K respectively, and **P** for the paramagnetic phase above 8 K. Changes occur because of the growth and shrinkage of magnetic Bragg peaks, and to changes in background intensity.

High resolution data were obtained using the diffractometer D2B at the ILL. All magnetic peaks in phase **A** are indexed by propagation vectors **k** = (0,0,1/2) and (1,0,1/2); the latter must be considered because of the centering of the cell.[24] In both cases the decomposition of the magnetic representations of the two

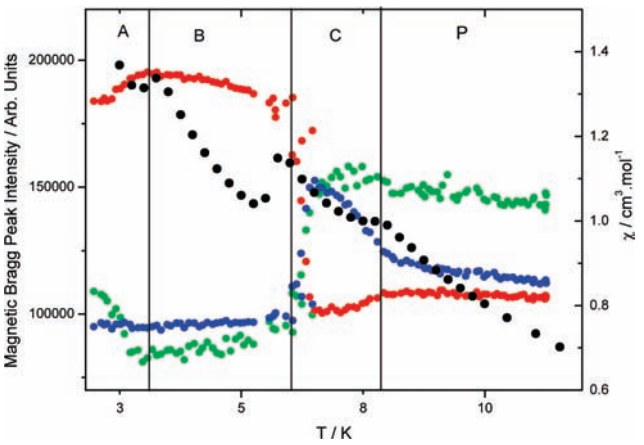

Figure 5. Superposition of the DC susceptibility data for **1** and the integrated intensity at various angles in the neutron diffraction pattern. Black, susceptibility; green, intensity between 8.9 and 10° 2θ; blue, intensity between 10 and 11.5° 2θ; red, intensity between 11.5 and 13.5° 2θ.

cobalt atoms are

$$\Gamma_{Co1} = 2\Gamma_2 + 1\Gamma_4$$

$$\Gamma_{Co2} = 1\Gamma_1 + 1\Gamma_2 + 2\Gamma_3 + 2\Gamma_4$$

However, it should be noted that the irreducible representations correspond to different structures for the two different propagation vectors. Four combinations of irreducible representations give good fits; considering both the goodness of fit, χ^2, and the magnitude of the moment, the structure is best described by the combination Co1 Γ_2, Co2 Γ_1. The moment magnitude has to be considered to ensure that the result does not correspond to unphysical magnetic structures. All possible combinations of basis vector for both propagation vectors, even those described by different irreducible representations, were refined in pairs to determine the true alignment of the moments (Figure 6, Figure S2, Supporting Information). This analysis shows that the structure is described fully by Co1 Γ_2 Ψ_2 and Co2 Γ_1 Ψ_1 with moments of 4.00(18) and 3.47(4) μ_B, respectively. The moments on Co2 align coparallel with each other and parallel to the b axis along the shared edge, with alternating edges aligned antiparallel to each other. The vertex sharing position (Co1) has the moment aligned along the c axis; as with the edge sharing positions, alternating positions align antiparallel to each other (Figure 7). Taking cross sections perpendicular to c at, for example, [a,b,0], [a,b,0.5], [a,b,1] shows that all

dx.doi.org/10.1021/ic101897a |*Inorg. Chem.* 2011, 50, 2246–2251

the Co2 sites have coparallel spins; equivalent slices at [a,b,0.25] and [a,b,0.75] show the Co1 spins within each layer also to be coparallel (Figure S3, Supporting Information).

There are notable differences in the diffraction pattern when the material enters phase **B**; the 0 1 0 reflection is no longer observed and the 0 0 1 magnetic Bragg peak is reduced in intensity. The structure of phase **B** was also investigated by examining all possible combinations of basis vectors. The moments on the Co2 site order with the same symmetry as in phase **A**, while the moment on Co1 consistently refines to zero (Figure 8). Comparison with the difference pattern shows a good agreement with the data (Figure 9).

The observation of a reduction in intensity and extra Bragg peaks is wholly consistent with this finding, as the large background change between phase **A** and phase **B** is indicative of the reduction of paramagnetic scattering of the unordered site and the additional Bragg peaks infer extra ordering.

Lack of order in materials with more than one magnetic site is referred to as idle spin behavior.[25,26] This phenomenon has been observed before in frustrated materials with more than one site, and previous explanations have been that only a portion of the sites order, so as to lessen frustration. To the authors' knowledge, no other spin idle compound has been found to undergo a further transition to a completely long-range ordered state upon cooling.

As with many other complex magnetic systems, even such well-studied examples as magnetite, it has not been possible to fully characterize all three phases to date. Attempts to solve the structure of the incommensurate phase, **C**, have so far been unsuccessful. Some relatively simple model structures can be eliminated, as we do not observe equally spaced incommensurate satellites around a central peak. Also the rate of incommensurability is different for different reflections. This is important as it implies that the structure is independently incommensurate in two different directions in reciprocal space. As such this phase is likely to be too complicated to be correctly solved using powder diffraction techniques, consequently single crystal neutron diffraction is planned.

Further neutron diffraction data using the high resolution diffractometer SPODI at the FRM II reveals the sensitivity of the magnetic structure to hydration level. On cooling below 170 K, intensity is observed in the diffraction pattern at positions expected for $hk \pm 1$ reflections which should be systematically absent, but indicate a doubling along *c*. Given that no similar change was reported in X-ray diffraction patterns[18] this can be ascribed to differences in positions of hydrogen atoms. Further interpretation of these changes is hampered by the lack of additional data represented by the observation of a small number of reflections and by the inaccuracy of the nuclear structure at this hydration level. Upon further cooling to phase **B**, we see a different magnetic diffraction pattern to previous experiments, notably the 001 is more intense and the 110 reflection is observed. Previous work[18] has proposed a large difference in magnetism upon going to the completely dehydrated structure; the current work suggests that changes in the magnetic structure can occur with only small changes to the level of dehydration.

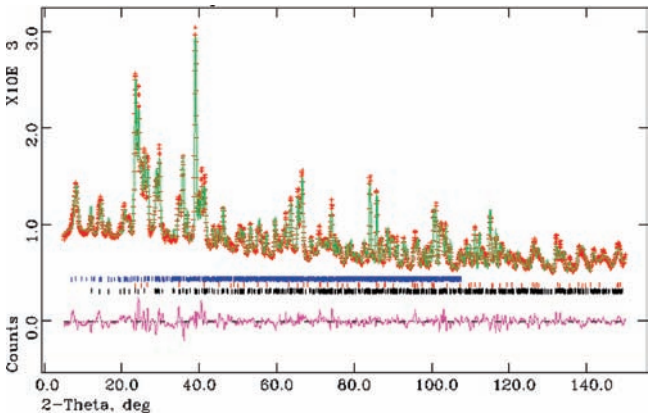

Figure 6. Rietveld refinement of the entire neutron diffraction pattern for phase **A** at 2 K using data from the D2B diffractometer. Black lines indicate allowed positions for nuclear Bragg peaks, blue marks for magnetic peaks, red marks show the allowed positions for ice Ih, which is present in small quantities as a consequence of the deuteration process.

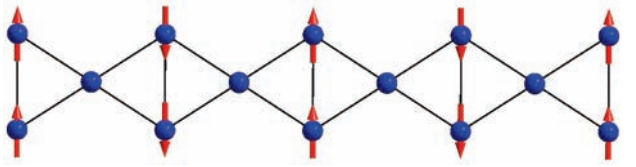

Figure 8. Magnetic structure of a chain in phase **B** at 3.5 K determined using neutron diffraction.

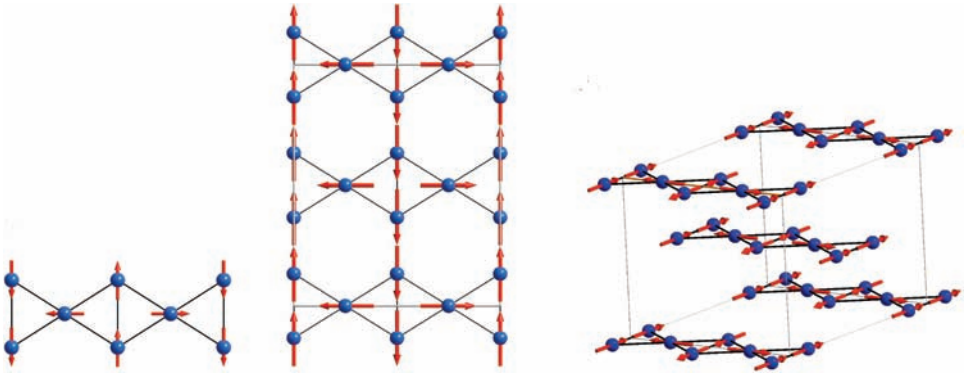

Figure 7. Magnetic structure of **1** at 2 K (i.e., in phase **A**). Left, one repeat unit in a single chain; center, three adjacent chains in the *bc* plane; right, one unit cell.

dx.doi.org/10.1021/ic101897a |*Inorg. Chem.* 2011, 50, 2246–2251

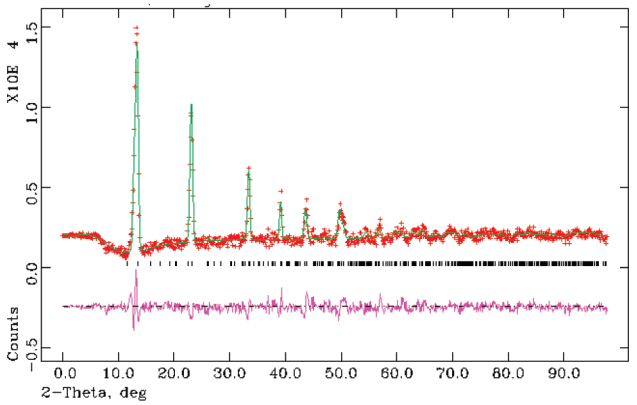

Figure 9. Magnetic-only Rietveld refinement for the neutron diffraction difference pattern (3.25 K−12 K).

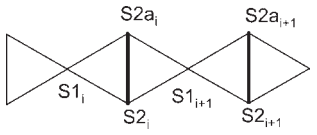

Figure 10. Exchange topology for **1**. Heavy lines represent J_1, faint J_2.

DISCUSSION

The magnetic structure of phase A shows an unusual mechanism for accommodating magnetic frustration. The structure of both phases A and B indicate that the Co2−Co2′ interaction (mediated by O3) is ferromagnetic, as seen in other Co(II) compounds with similar exchange pathways,[27−29] and that the next-nearest neighbor Co2−Co2″ interaction (mediated by O1−C1−C2−O2) is antiferromagnetic. As shown in Figure 10, the spin on Co1 cannot now order in such a way as to satisfy the Co1−Co2 exchange interaction irrespective of whether this interaction is ferro- or antiferromagnetic. The observation of a structure in which the spin on Co1 orders orthogonal to those on Co2 indicates the importance of single ion anisotropy leading to an antisymmetric (Dzyaloshinskii−Moriya) contribution to the spin Hamiltonian. This stabilizes the orthogonal arrangement, and in the presence of frustration of the symmetric exchange interactions it is possible that this can dominate the observed structure.

On heating, a magnetic phase transition occurs to a structure in which the spin on Co1 is not ordered. This *idle spin* behavior has previously been observed when geometric frustration is present in an extended lattice of reasonable high symmetry. Nearest neighbor exchange interactions to Co1 provide no enthalpic driving force for ordering; hence, long-range order must be the result of next-nearest (or further) interactions which will necessarily be weak. This enthalpic contribution will be easily overcome, even at low temperatures, by the entropy increase associated with loss of order.

We can rationalize the presence of multiple phase transitions by considering the types of behavior we can expect for different relative sizes of the parameters in the simplified Hamiltonian (eq 1):

$$\hat{H} = -J_1 \sum_i S2_i \cdot S2a_i - J_2 \sum_i (S1_i \cdot S2_i + S1_i \cdot S2_{i+1}) + \sum_i (D_1 S1_i^2 + D_2 S2_i^2) \quad (1)$$

To derive some meaningful results we have to consider only nearest neighbor interactions and consider that the zero-field splitting is no higher than tetragonal. We can then contemplate two limiting cases:[30] $D>J$ and $J>D$. In the first case, the two sites will behave independently; hence, the ordering of the individual sites does not have to be described by the same irreducible representation, and the sites may order at different temperatures. In the second case, there is strong coupling between the sites leading to a single phase transition and a structure where the basis vectors for the spins on both sites must belong to the same irreducible representation.

The need for two irreducible representations to describe phase A indicates that single ion anisotropy is the dominant factor in determining the magnetic structure. This situation should give only two ordered phases, but we observe three, indicating that the relationship between J and D is not straightforward. In this particular case, we postulate that all four parameters in the Hamiltonian; D_1, D_2, J_1, and J_2 have similar magnitudes. This allows us to tentatively suggest the following mechanism for the transitions to phases **A**, **B**, and **C**. At 8 K, the moments order according to the symmetry as determined by single ion effects of Co2. As the temperature is lowered, the effect of the exchange interaction is to perturb the ordered structure; initially this causes the observed incommensurability, however, at 6.2 K this becomes critical and phase **B** is observed. The final phase transition is caused by the ordering of the moments of Co1; the temperature of this transition is suppressed because of the frustration inherent in the ordering of Co2. This exchange topology has been studied theoretically in the case of mixed S and mixed anisotropy systems. Depending on the ratio of anisotropy to exchange interactions, different ground states are predicted.[31]

CONCLUSION

We have shown that neutron diffraction is a powerful tool for helping to elucidate the behavior of magnetic coordination networks, just as it is for metal oxides. In addition, the greater range of structure types available for coordination networks indicates that many new types of magnetic structure may be discovered for them using this technique.

ASSOCIATED CONTENT

Supporting Information. Powder X-ray diffraction refinement, refinement graphs for selected mixing coefficients and an additional view of the magnetic structure. This material is available free of charge via the Internet at http://pubs.acs.org.

AUTHOR INFORMATION

Corresponding Author

*E-mail: ptw22@cam.ac.uk.

Present Addresses

◆Helmholtz-Zentrum Berlin für Materialen und Energie GmbH, Glienickerstrasse 100, 14109 Berlin, Germany.

ACKNOWLEDGMENT

We thank the UK EPSRC for a studentship (R.A.M.) and a senior fellowship (P.R.R.). This research project has been supported by the European Commission under the seventh Framework Program through the 'Research Infrastructures' action of the 'Capacities' Program, Contract No. CP-CSA_INFRA-2008-1.1.1 Number 226507-N MI3, the MAGMANet Network of Excellence

of the E.U., the Spanish MEC (Projects MAT2007-61584, CSD 2007-00010 Consolider-Ingenio in Molecular Nanoscience and a Ramon y Cajal fellowship for A.A.) and the Generalitat Valenciana (Project PROMETEO/2009/095). We also thank staff at the ILL and FRM II for technical help.

REFERENCES

(1) Robson, R. *Dalton Trans.* 2008, 5113.
(2) Cheetham, A. K.; Rao, C. N. R.; Feller, R. K. *Chem. Commun.* 2006, 4780.
(3) Kitagawa, S.; Kitaura, R.; Noro, S. *Angew. Chem., Int. Ed.* 2004, *43*, 2334.
(4) Dinca, M.; Long, J. R. *Angew. Chem., Int. Ed.* 2008, *47*, 6766.
(5) Peterson, V. K.; Liu, Y.; Brown, C. M.; Kepert, C. J. *J. Am. Chem. Soc.* 2006, *128*, 15578.
(6) Yildirim, T.; Hartman, M. R. *Phys. Rev. Lett.* 2005, *95*, 215504.
(7) Dinca, M.; Dailly, A.; Liu, Y.; Brown, C. M.; Neumann, D. A.; Long, J. R. *J. Am. Chem. Soc.* 2006, *128*, 16876.
(8) Rowsell, J. L. C.; Eckert, J.; Yaghi, O. M. *J. Am. Chem. Soc.* 2005, *127*, 14904.
(9) Forster, P. M.; Eckert, J.; Heiken, B. D.; Parise, J. B.; Yoon, J. W.; Jhung, S. H.; Chang, J.-S.; Cheetham, A. K. *J. Am. Chem. Soc.* 2006, *128*, 16846.
(10) Miller, J. S.; Drillon, M. *Magnets: Molecules to Materials V*; Wiley VCH: Weinheim, Germany, 2004.
(11) Grohol, D.; Matan, K.; Cho, J.-H.; Lee, S.-H.; Lynn, J. W.; Nocera, D. G.; Lee, Y. S. *Nat. Mater.* 2005, *4*, 232.
(12) Lee, S. H.; Broholm, C.; Ratcliffe, W.; Gasparovic, G.; Huang, Q.; Kim, T. H.; Cheong, S. W. *Nature* 2002, *418*, 857.
(13) Blundell, S. J. *Contemp. Phys.* 1999, *40*, 175.
(14) Mole, R. A.; Stride, J. A.; Unruh, T.; Wood, P. T. *J. Phys.: Condens. Matter* 2009, *21*, 076003.
(15) Mole, R. A.; Stride, J. A.; Wills, A. S.; Wood, P. T. *Phys. B* 2006, *385*, 435.
(16) Yufit, D. S.; Price, D. J.; Howard, J. A. K.; Gutschke, S. O. H.; Powell, A. K.; Wood, P. T. *Chem. Commun.* 1999, 1561.
(17) Gutschke, S. O. H.; Molinier, M.; Powell, A. K.; Wood, P. T. *Angew. Chem., Int. Ed. Engl.* 1997, *36*, 991.
(18) Kurmoo, M.; Kumagai, H.; Chapman, K. W.; Kepert, C. J. *Chem. Commun.* 2005, 3012.
(19) Larson, A. C.; Von Dreele,R. B. *General Structure Analysis System (GSAS)*, Los Alamos National Laboratory Report LAUR 86-748, 1994.
(20) Wills, A. S. *Phys. B* 2000, *276*, 680.
(21) Carlin, R. L. *Magnetochemistry*; Springer-Verlag: Berlin, Germany, 1986.
(22) Van Vleck, J. H. *Physica* 1973, *69*, 177.
(23) Hansen, T. C.; Henry, P. F.; Fischer, H. E.; Torregrossa, J.; Convert, P. *Meas. Sci. Technol.* 2008, *19*, 034001.
(24) Wills, A. S. *Z. Kristallogr.* 2007, *26* (Suppl.), 56.
(25) Leblanc, M.; Ferey, G.; Calage, Y.; De Pape, R. *J. Solid State Chem.* 1984, *53*, 360.
(26) Aranda, M. A. G.; Attfield, J. P.; Batchelor, E.; Shields, G. P.; Bruque, S.; Gabás, M. *Inorg. Chem.* 1998, *37*, 1329.
(27) Barandika, M. G.; Serna, Z.; Cortés, R.; Lezama, L.; Urtiaga, M. K.; Arriortua, M. I.; Rojo, T. *Chem. Commun.* 2001, 45.
(28) Serna, Z. E.; Urtiaga, M. K.; Barandika, M. G.; Cortés, R.; Martin, S.; Lezama, L.; Arriortua, M. I.; Rojo, T. *Inorg. Chem.* 2001, *40*, 4550.
(29) Rojo, J. M.; Mesa, J. L.; Lezama, L.; Pizarro, J. L.; Arriortua, M. I.; Fernandez, J. R.; Barberis, G. E.; Rojo, T. *Phys. Rev. B* 2002, *66*, 094406.
(30) Bertaut, E. F. *J. Phys., Colloq.* 1971, *C1*, 462.
(31) Čanova, L.; Strečka, J.; Jaščur, M. *J. Phys.: Condens. Matter* 2006, *18*, 4967.